Spontaneous chiralization of polar active particles

Marco De Corato [*]
Aragon Institute of Engineering Research (I3A), University of Zaragoza, 50009 Zaragoza, Spain

Ignacio Pagonabarraga [†]
Departament de Física de la Matèria Condensada, Universitat de Barcelona, C. Martí Franquès 1, 08028 Barcelona, Spain
University of Barcelona Institute of Complex Systems (UBICS), Universitat de Barcelona, 08028 Barcelona, Spain
and CECAM, Centre Européen de Calcul Atomique et Moléculaire, École Polytechnique Fédérale de Lausanne (EPFL), Batochime, Avenue Forel 2, 1015 Lausanne, Switzerland

Giovanniantonio Natale [‡]
Department of Chemical and Petroleum Engineering, University of Calgary, 2500 University Drive NW, Calgary, Canada

(Received 21 January 2021; revised 20 September 2021; accepted 26 September 2021; published 15 October 2021)

Polar active particles constitute a wide class of active matter that is able to propel along a preferential direction, given by their polar axis. Here, we demonstrate a generic active mechanism that leads to their spontaneous chiralization through a symmetry-breaking instability. We find that the transition of an active particle from a polar to a chiral symmetry is characterized by the emergence of active rotation and of circular trajectories. The instability is driven by the advection of a solute that interacts differently with the two portions of the particle surface and it occurs through a supercritical pitchfork bifurcation.

DOI: 10.1103/PhysRevE.104.044607

I. INTRODUCTION

The development of engineered active colloids that harness the chemical energy of the environment to move [1–3] has enabled one to mimic and dissect mechanisms in biological systems while opening doors to multiple applications: bioremediation, micromixing, micromachinery, drug delivery, and more [4–10]. To imitate the intrinsic asymmetry of flagellates and other microorganisms, active colloids are designed with fore-aft asymmetric chemical activity, which defines their polar axis and their preferential direction of motion [11,12]. Alternatively, in the absence of a built-in asymmetry, a polar axis defining the direction of motion of an isotropic active particle can emerge from a spontaneous symmetry-breaking instability [13–19] that is reminiscent of that used by cells to migrate [20–22]. However, unlike their biological counterparts that have evolved internal mechanochemical processes to actively change the direction of motion [23], active colloids can only rely on passive rotational diffusion [12]. Providing them with active rotation requires breaking the polar symmetry through the use of external fields, external gradients, the presence of confining walls, or by designing them with a chiral shape or with a chiral chemical activity [24–36]. The resulting self-rotation has been exploited to develop autonomous sorting of active particles [37–40] and also as a potential solution to move barriers or micromachinery [41,42].

Recent experiments and simulations showed that Janus active particles and active droplets can spontaneously break their polar symmetry and transition from a persistent Brownian motion with enhanced rotational diffusion [43–48] to circular [49] or helical trajectories [50,51]. Such a symmetry-breaking instability could offer a controllable way to trigger active rotation, which does not require a built-in chiral shape nor a chiral chemical activity. In this article, we demonstrate that chiral motion is a generic feature of polar active particles moving through a solute. It occurs via an advective instability that requires two ingredients only: (i) repulsive and attractive solute-surface interactions along the direction of motion, and (ii) an active mechanism that generates a dipolar distribution of solute.

The spontaneous chiralization mechanism is schematically depicted in Fig. 1. A spherical particle generates a solute concentration gradient through an active mechanism. The interaction between the solute and the surface of the particle introduces a body force $\boldsymbol{f} = c\,\nabla\phi$ in the fluid. In Figs. 1(a) and 1(c) the particle does not rotate because the configuration is left-right symmetric. A transient perturbation of the polar vector leads to a configuration where $\boldsymbol{f}$ applies a torque to the fluid, which is balanced by an opposite torque on the particle [see Figs. 1(b) and 1(d)]. If the torque is directed as in Fig. 1(b) and the solute diffusion is slower than the advection, then the initial perturbation is reinforced, the active particle keeps rotating, and the polar symmetry breaks. Conversely, if the torque is directed as in Fig. 1(d), the initial configuration is restored.

II. ACTIVE PARTICLE MODEL AND GOVERNING EQUATIONS

To illustrate the generality of the symmetry-breaking mechanism, we employ a mathematical model that describes

[*]mdecorato@unizar.es
[†]ipagonabarraga@ub.edu
[‡]gnatale@ucalgary.ca

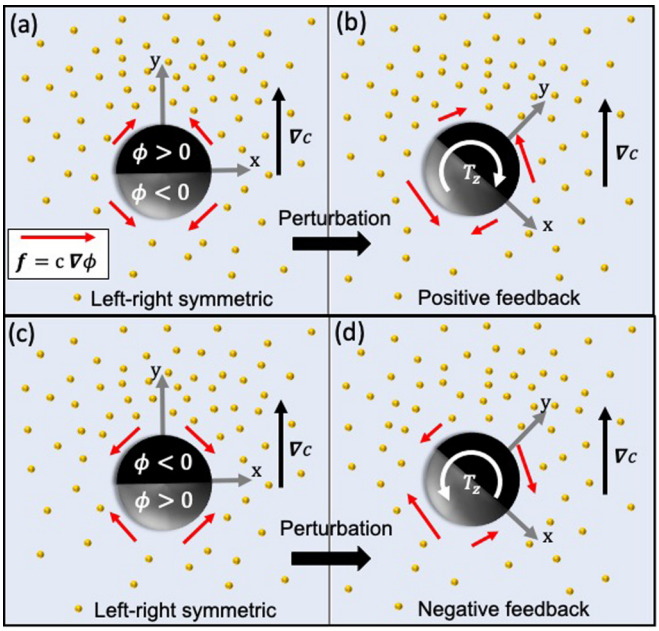

FIG. 1. Schematics of the spontaneous chiralization mechanism; the translational velocity is not shown for clarity. (a) and (c) An active particle with attractive ($\phi < 0$) and repulsive ($\phi > 0$) solute-surface interactions on the two hemispheres generates a concentration dipole through an active mechanism. The solute-surface interactions generate a body force $\boldsymbol{f}$ in the fluid. (b) and (d) A perturbation of the polar axis changes $\boldsymbol{f}$, which applies a torque to the fluid. The torque on the fluid must be balanced by an opposite torque on the particle. In (b), this leads to a clockwise rotation, which reinforces the initial perturbation possibly breaking the left-right symmetry if the solute diffusion is slower than the advection due to the rotating flow. In (d), the torque is reversed and the rotation restores the initial configuration.

two propulsion mechanisms: squirmers [52] and chemically active particles [53]. We consider a spherical particle of radius R that is suspended in a Newtonian and incompressible liquid of shear viscosity η that contains a solute. We employ a corotating Cartesian reference frame with the origin at the particle center. Without any loss of generality, we choose the y axis to be aligned with the polar axis of the particle (see Fig. 1).

In the corotating reference frame, the steady-state solute concentration c obeys

$$D\nabla\cdot\left(\nabla c + c\nabla\frac{\phi}{k_BT}\right) = \boldsymbol{v}\cdot\nabla c, \tag{1}$$

with $\boldsymbol{v}$ the fluid velocity, D the solute diffusion coefficient, k_BT the thermal energy, and ϕ the interaction potential between the solute and the particle surface. The potential energy ϕ decays with the separation from the surface and changes from attractive to repulsive along y. It can be written as $\phi = \phi_0\, g(y/r)h(r/R)$, where $h(r/R)$ determines how quickly it decays to zero far from the surface, $g(y/R)$ determines its changes along y, and r denotes the distance from the particle center. To model chemically active particles, we assume that the solute is released or consumed at $r = R$ through a surface flux density given by $\boldsymbol{n}\cdot(\nabla c + c\nabla\phi/k_BT) = -Q\, f(y/R)/D$, with $\boldsymbol{n}$ the vector normal to the particle surface pointing outwards. The magnitude of the solute flux density is Q, and the function $f(y/R)$ determines its distribution. The solute is released if $f(y/R) > 0$ while it is consumed if $f(y/R) < 0$. Far from the particle the solute concentration is $c = c_\infty$.

The velocity and pressure fields satisfy the Stokes equations

$$\nabla\cdot\boldsymbol{\sigma} = \eta\nabla^2\boldsymbol{v} - \nabla p = \boldsymbol{f}, \quad \nabla\cdot\boldsymbol{v} = 0, \tag{2}$$

with $\boldsymbol{\sigma}$ the stress tensor for a Newtonian fluid and $\boldsymbol{f} = c\nabla\phi$ is the body force due to the solute-wall interactions. To model the propulsion of particles via a general mechanism, we use the squirmer model, which postulates a steady slip velocity $\boldsymbol{v} = B_1\,\hat{\boldsymbol{y}}\cdot(\boldsymbol{I} - \boldsymbol{nn})$ at $r = R$ [52], where $\hat{\boldsymbol{y}}$ is the y-axis unit vector and B_1 specifies the slip velocity magnitude. In the corotating frame, the boundary conditions at $r \to \infty$ are given by $\boldsymbol{v} = -\boldsymbol{V} - \boldsymbol{\omega}\times\boldsymbol{r}$, where $\boldsymbol{V}$ and $\boldsymbol{\omega}$ are the translational and rotational velocity of the particle, respectively.

Equations (1) and (2) are completed by the balance of linear and angular momentum on the particle. By neglecting inertia and Brownian forces, they read

$$\int_S \boldsymbol{\sigma}\cdot\boldsymbol{n}\, dS = -\int_\Omega \boldsymbol{f}\, d\Omega, \tag{3}$$

$$\int_S \boldsymbol{r}\times\boldsymbol{\sigma}\cdot\boldsymbol{n}\, dS = -\int_\Omega \boldsymbol{r}\times\boldsymbol{f}\, d\Omega, \tag{4}$$

where S denotes the particles surface and Ω the volume outside the sphere. Equations (1)–(4) describe chemically active particles when $Q \neq 0$ and $B_1 = 0$ and squirmers when $Q = 0$ and $B_1 \neq 0$. In this way, we study the stability of the polar propulsion regime and the onset of chirality using two distinct within a single framework. The equations are solved using the finite-element software COMSOL [54]. To investigate the stability of the polar and chiral propulsion regimes, we perform a parametric continuation study of the steady-state solution branches. The set of parameters that yield steady states with $\boldsymbol{\omega} \neq \boldsymbol{0}$ represent chiral states whereas polar states are characterized by $\boldsymbol{\omega} = \boldsymbol{0}$ and $\boldsymbol{V}$ directed along y.

III. SPONTANEOUS CHIRALIZATION OF CHEMICALLY ACTIVE PARTICLES

To illustrate the spontaneous chiralization of chemically active particles, we investigate a simple realization of Fig. 1. We assume that the solute concentration is zero at infinity $c_\infty = 0$ and that the chemical activity changes linearly along the polar axis of the active particle $f(y/R) = y/R$. To simplify the numerical solution, we assume that the interaction potential decays to zero over a small distance from the surface and we use the phoretic framework [54]. This standard simplification has been employed in multiple previous works on chemically active particles [53]. Under this assumption, the solute-surface interactions are characterized by the phoretic mobility coefficient, $\tilde{M}(y/R) = k_BT/\eta\int_R^\infty (r - R)[\exp(\phi/k_BT) - 1]dr$, which is positive for repulsive interactions and negative for attractive interactions [55]. In this example, we assume that $\tilde{M}(y/R) = My/R$ with $M > 0$, which corresponds to repulsive interactions for $y > 0$ and attractive for $y < 0$. This problem displays a single dimensionless parameter, $\overline{Q} = QRM/D^2$, which determines the importance of advection over diffusion and it is equivalent to

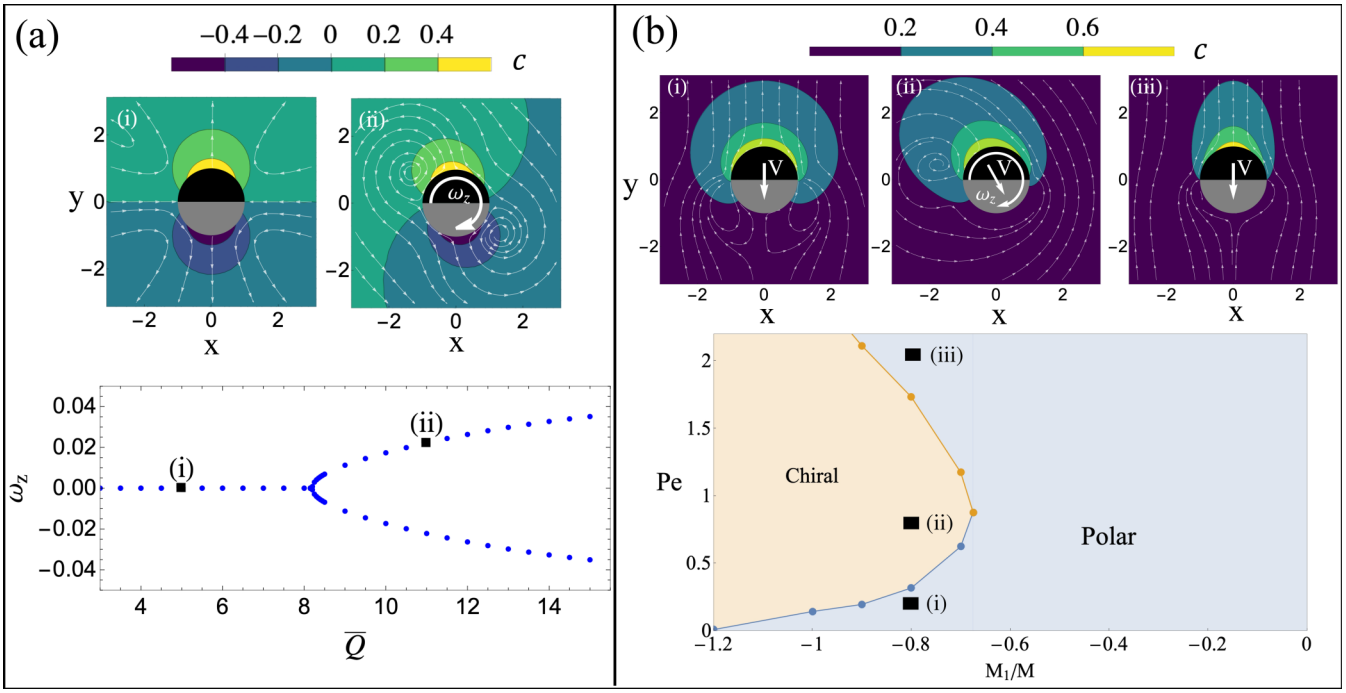

FIG. 2. (a) The rotation rate of a chemically active particle made dimensionless using the characteristic time QM/RD in the case of $f(y/R) = y/R$ and $\tilde{M}(y/R) = My/R$. At small values of $\overline{Q}$, the concentration profile is left-right symmetric and aligned with the polar axis of the particle. At large values of $\overline{Q}$, the polar symmetry breaks and the particle starts to rotate. Insets: The distribution of solute and the streamlines in the symmetry plane $z = 0$. (b) Phase diagram of the behavior of a chemically active Janus particle as a function of Pe and of M_1/M. The upper figures show the steady-state solute distribution and the streamlines in the symmetry plane $z = 0$.

a Péclet number, evaluated using QM/D as the characteristic velocity [56]. Another computational advantage of this illustrative example is that the active particle behaves as a shaker: It does not translate but it generates recirculating flows [57].

In Fig. 2(a), we plot the steady-state value of ω_z as a function of $\overline{Q}$. The stationary polar configuration undergoes a supercritical pitchfork bifurcation becoming unstable. For $\overline{Q}$ larger than a critical value, the particle spontaneously rotates about the z axis through the mechanism depicted schematically in Figs. 1(a) and 1(b). The insets of Fig. 2(a) show the solute distribution and streamlines around the particle in the polar and in the chiral steady states. The instability is prevented if the solute is attracted to the surface where it is released, $\tilde{M}(y/R) = -My/r$, corresponding to Figs. 1(c) and 1(d). In this case, numerical simulations reveal that the stationary state is stable.

The active particle described so far highlights the essential nature of the self-chiralization. However, chemically active particles self-propel when the chemical activity and solute-surface interactions vary independently. To understand the effect of self-propulsion on the emergence of chiral states, we consider a Janus particle. The solute is released only from one hemisphere, specifically $f(y/R) = \Theta(y/R)$ where Θ is the Heaviside theta function, and experiences repulsive interactions with the catalytic hemisphere, $\tilde{M}(y/R) = M$ for $y > 0$, and is either attracted or repelled by the inactive hemisphere, $\tilde{M}(y/R) = M_1$ for $y < 0$. We are interested in cases when $M_1/M < 0$ and the solute is attracted by the chemically inactive surface. The direction of motion of the active particle is determined by the sign of $1 - M_1/M$ [30,56,57].

Figure 2(b) summarizes the behavior of a freely suspended Janus particle as a function of the Péclet number $\mathrm{Pe} = VR/D$, evaluated with the magnitude of the velocity V and of the phoretic mobility ratio M_1/M. Note that the translational velocity used in the Péclet number is a result of the simulation, and we control it by increasing or decreasing the surface flux of solute Q. The solution map, shown in Fig. 2(b), displays a region where the polar symmetry is stable and a region in which the polar symmetry spontaneously breaks and the active particle becomes chiral. In the chiral regime, the active particle translates and rotates, and its trajectory, observed from a fixed frame, changes from straight to circular. At large Pe, Fig. 2(b) shows a reentrant polar regime where the polar symmetry is restored. In this regime, the translational motion of the particle advects the solute away from the face that is chemically inert, as shown in Fig. 2(iii). In this case, most of the solute concentrates in the wake behind the active particle, hindering the flows due to the solute-surface interactions. This stabilizes the propulsion of the particle along its polar vector.

IV. SPONTANEOUS CHIRALIZATION OF SQUIRMERS

Next, we show that the same symmetry-breaking mechanism discussed for chemically active particles drives the spontaneous chiralization of squirmers. In this case, there is no chemical reaction $Q = 0$, instead, the particle moves through a solution of a given concentration c_∞. The solute interacts with the particle surface through the potential $\phi = \phi_0(y/r - 1/2)\exp[-\lambda(r - R)]$, with λ^{-1} setting the characteristic interaction distance. The interaction is repulsive

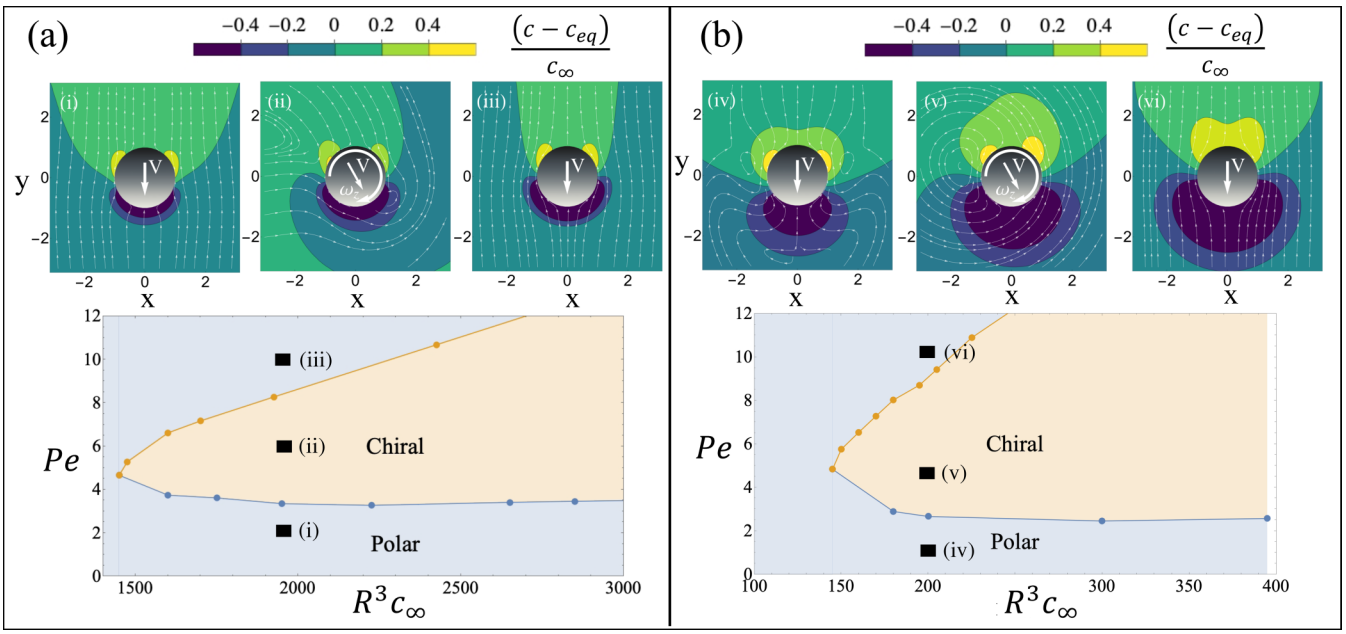

FIG. 3. Propulsion regimes of a squirmer moving through a solution of concentration c_∞. The solute-surface interactions are given by $\phi = \phi_0(y/r - 1/2)\exp[-\lambda(r-R)]$, which is repulsive for $y/r > -1/2$ and attractive for $y/r < -1/2$. (a) Short-ranged potential $\lambda = 5/R$ and $\phi_0 = 1.5k_BT$ and (b) range of the potential comparable to the particle size $\lambda = 1/R$ and $\phi_0 = k_BT$. The upper figures display the deviation of c from its equilibrium distribution $c_{\rm eq}$ and the flow streamlines in the symmetry plane $z = 0$.

for $y/r > -1/2$ and attractive for $y/r < -1/2$. We study the case where the active flow generated by the squirmer drives a concentration gradient by advecting the solute away from the attractive side and accumulating on the repulsive side of the particle surface, $B_1 < 0$. We perform numerical simulations solving for the steady states that have a nonzero ω_z, which represent chiral states, and use a numerical continuation to reconstruct the solution branches and the bifurcations.

In Fig. 3(a) we report the solution map for a short-ranged and relatively weak potential, $\lambda = 5/R$ and $\phi_0 = 1.5k_BT$. We find that the chiral regime extends over a broad range of solute concentration c_∞ and Péclet numbers $\mathrm{Pe} = VR/D$. To control the Péclet number in these simulations, we change the squirming parameter B_1. By increasing Pe at a fixed value of c_∞, the squirmer undergoes a supercritical bifurcation acquiring a rotation rate. Similar to the case of chemically active particles, at large Pe, the chiral regime becomes unstable and we find a reentrant polar regime. In Fig. 3(b), we show that considering a larger interaction range $\lambda = 1/R$ and a slightly smaller potential energy $\phi_0 = k_BT$ results in a solution map that is qualitatively similar to that shown in Fig. 3(a). By comparing Figs. 3(a) and 3(b) it is apparent that the value of Pe at which the spontaneous chiralization occurs is roughly the same but it occurs at a smaller solute concentration c_∞ in the case of Fig. 3(b). In Figs. 3(i)–3(vi) we report the flow field and the deviation of the solute distribution from that at equilibrium, $(c - c_{\rm eq})/c_\infty$, with $c_{\rm eq} = c_\infty \exp(-\phi/k_BT)$. Figures 3(i) and 3(iv) reveal that, before the onset of the chiral regime, the solute is being transported towards the side with repulsive interactions, $y/r > -1/2$, by the active flows. This confirms that the mechanism driving the symmetry-breaking instability is the same for squirmers and for chemically active particles.

V. COMPARISON WITH EXPERIMENTS

The spontaneous chiralization of a squirmer can be compared to recent experiments using active Janus particles in a polymer solution [49]. In the experiments of Narinder *et al.* [49], a silica particle of radius $R \approx 4\ \mu$m and half coated with carbon, moves through a polymer, polyacrylamide (PAAm), suspended in a mixture of water and propyleneglycol *n*-propyl ether (PnP) that is near the critical temperature. The colloid is illuminated by a laser that increases the temperature of the carbon coating above the unmixing temperature, which drives the phase separation of water and PnP. The phase separation propels the active colloid through the polymer suspension. Above a critical translational velocity, $V \approx 0.25\ \mu\mathrm{m\,s^{-1}}$, the active particle acquires a rotation rate and transitions from straight to circular trajectories. We argue that the symmetry-breaking instability observed in these experiments displays all the ingredients required by our theory to observe a transition from polar states to chiral states, namely, (i) a solute that experiences attractive and repulsive interactions with different portions of the surface of the active colloid, and (ii) an active mechanism that generates a solute gradient.

To connect our model to the experiments, we assume that the polymer distribution is described by the solute field c. Using typical values of diffusion coefficients for high-molecular-weight polymers $D \approx 0.1$–$1\ \mu\mathrm{m^2\,s^{-1}}$, the particle radius $R \approx 4\ \mu$m, the velocity $V \approx 0.25\ \mu\mathrm{m\,s^{-1}}$, and the polymer concentration, we estimate the experimental Péclet number as $\mathrm{Pe} = VR/D \approx 1$–$10$ and the experimental dimensionless number density $c_\infty R^3 \approx 1000$ [54]. These values are within the range where Fig. 3 predicts the transition to the chiral state. The PAAm polymers used in Ref. [49] are highly hydrophilic and their interactions with the particle surface

are attractive at the hydrophilic silica side and repulsive at the hydrophobic carbon side, similarly to our model. More details on the polymer-surface interactions can be found in Ref. [54]. Besides the direct surface-PAAm interactions discussed above, the solvent unmixing generates a nonpolar (PnP) droplet near the carbon surface [58] in which the PAAm polymers are not easily dissolved. The PAAmn polymer chains are repelled from the PnP droplet, which should further contribute to the repulsive polymer-surface interactions near the carbon hemisphere. The solvent phase separation also generates a gradient of nonpolar molecules (PnP) between the carbon and the silica side, with more polar molecules near the silica side. The PAAm polymers prefer the interactions with the polar molecules (water) and therefore they are attracted towards areas of small PnP concentration, that is, towards the silica hemisphere. In summary, it can be argued that the solvent unmixing taking place in the experiments of Narinder *et al.* should further contribute to the repulsive interactions with the carbon side and with attractive interactions with the silica side. Finally, in Ref. [49] the active particle moves towards the side with attractive solute-surface interactions, the silica, in agreement with our findings shown in Fig. 3. To rule out the hypothesis that the experimental observations are caused by a viscoelastic instability, we computed the Deborah number, $\mathrm{De} = V\tau/R$, which represents the product of the characteristic shear rate and the relaxation time of the polymers, τ. The authors report $\tau \approx 1.6$ s [43], which yields $\mathrm{De} \approx 0.1$. This value is much smaller than that for which elastic instabilities have been reported [59–61] and for similar values of De the active particles used in Ref. [62] did not transition to chiral states.

VI. SUMMARY AND CONCLUSIONS

We demonstrate that chirality spontaneously arises for polar active particles that attract and repel a solute on two different portions of its surface. Above a critical Péclet number, the polar symmetry is broken and the particle acquires a steady rotation rate. The only required ingredient is an active mechanism that accumulates solutes on the repulsive side and depletes it from the attractive one. The specific nature of the active mechanism driving the concentration gradient appears to be irrelevant. Since the active particle models used here have been successfully employed to study synthetic [63,64] and biological active matter [65], we expect the results to be relevant for a wide class of systems. Indeed, we illustrated this transition by considering chemically active colloids and squirmers, but we expect that other active mechanisms that generate solute gradients would display qualitatively similar behavior, as long as the solute interacts differently with the two sides of the particle.

ACKNOWLEDGMENTS

M.D.C. acknowledges funding from the European Union's Horizon 2020 research and innovation program under the Marie Skłodowska-Curie action (GA 712754), the Severo Ochoa program (SEV-2014-0425), the CERCA Programme/Generalitat de Catalunya, and from the Ministerio de Cierncia e Innovación (MCIN) through the Juan de la Cierva Incorporación postdoctoral fellowship ICJ2018-035270-I. I.P. acknowledges support from MINECO Project No. PGC2018-098373-B-I00, from the DURSI Project No. 2017SGR-884, from the SNF Project No. 200021-175719, and from the EU Horizon 2020 program through 766972-FET-OPEN NANOPHLOW. G.N. acknowledges the support of the Natural Sciences and Engineering Research Council of Canada (NSERC) Discovery Grant No. RGPIN-2017-03783. M.D.C wishes to acknowledge useful discussions with Gaetano D'Avino, Francesco Greco, and Pier Luca Maffettone. The authors thank Valeria Garbin and Raymond Kapral for valuable feedback on an earlier version of the manuscript. The authors wish to thank the anonymous reviewers for their suggestions that significantly improved the manuscript.

[1] D. Needleman and Z. Dogic, Nat. Rev. Mater. **2**, 17048 (2017).
[2] A. Zöttl and H. Stark, J. Phys.: Condens. Matter **28**, 253001 (2016).
[3] P. Illien, R. Golestanian, and A. Sen, Chem. Soc. Rev. **46**, 5508 (2017).
[4] S. Das, A. Garg, A. I. Campbell, J. Howse, A. Sen, D. Velegol, R. Golestanian, and S. J. Ebbens, Nat. Commun. **6**, 8999 (2015).
[5] C. Maggi, J. Simmchen, F. Saglimbeni, J. Katuri, M. Dipalo, F. De Angelis, S. Sanchez, and R. Di Leonardo, Small **12**, 446 (2016).
[6] Z. Huang, P. Chen, G. Zhu, Y. Yang, Z. Xu, and L.-T. Yan, ACS Nano **12**, 6725 (2018).
[7] J. Parmar, D. Vilela, K. Villa, J. Wang, and S. Sánchez, J. Am. Chem. Soc. **140**, 9317 (2018).
[8] A. C. Hortelão, R. Carrascosa, N. Murillo-Cremaes, T. Patiño, and S. Sánchez, ACS Nano **13**, 429 (2018).
[9] L. Wang, S. Song, J. van Hest, L. K. E. A. Abdelmohsen, X. Huang, and S. Sánchez, Small **16**, 1907680 (2020).
[10] S. Tang, F. Zhang, H. Gong, F. Wei, J. Zhuang, E. Karshalev, B. E.-F. de Ávila, C. Huang, Z. Zhou, Z. Li *et al.*, Sci. Robot. **5**, eaba6137 (2020).
[11] W. F. Paxton, K. C. Kistler, C. C. Olmeda, A. Sen, S. K. St. Angelo, Y. Cao, T. E. Mallouk, P. E. Lammert, and V. H. Crespi, J. Am. Chem. Soc. **126**, 13424 (2004).
[12] J. R. Howse, R. A. L. Jones, A. J. Ryan, T. Gough, R. Vafabakhsh, and R. Golestanian, Phys. Rev. Lett. **99**, 048102 (2007).
[13] P. de Buyl, A. S. Mikhailov, and R. Kapral, Europhys. Lett. **103**, 60009 (2013).
[14] S. Michelin, E. Lauga, and D. Bartolo, Phys. Fluids **25**, 061701 (2013).
[15] Z. Izri, M. N. van der Linden, S. Michelin, and O. Dauchot, Phys. Rev. Lett. **113**, 248302 (2014).
[16] C. C. Maass, C. Krüger, S. Herminghaus, and C. Bahr, Annu. Rev. Condens. Matter Phys. **7**, 171 (2016).
[17] D. Boniface, C. Cottin-Bizonne, R. Kervil, C. Ybert, and F. Detcheverry, Phys. Rev. E **99**, 062605 (2019).

[18] W.-F. Hu, T.-S. Lin, S. Rafai, and C. Misbah, Phys. Rev. Lett. **123**, 238004 (2019).

[19] M. De Corato, I. Pagonabarraga, . K. E. A. Abdelmohsen, S. Sánchez, and M. Arroyo, Phys. Rev. Fluids **5**, 122001(R) (2020).

[20] V. Ruprecht, S. Wieser, A. Callan-Jones, M. Smutny, H. Morita, K. Sako, V. Barone, M. Ritsch-Marte, M. Sixt, R. Voituriez, and C.-P. Heisenberg, Cell **160**, 673 (2015).

[21] A. C. Callan-Jones, V. Ruprecht, S. Wieser, C. P. Heisenberg, and R. Voituriez, Phys. Rev. Lett. **116**, 028102 (2016).

[22] A. Farutin, J. Étienne, C. Misbah, and P. Recho, Phys. Rev. Lett. **123**, 118101 (2019).

[23] K. Son, J. S. Guasto, and R. Stocker, Nat. Phys. **9**, 494 (2013).

[24] D. J. Kraft, R. Wittkowski, B. ten Hagen, K. V. Edmond, D. J. Pine, and H. Löwen, Phys. Rev. E **88**, 050301(R) (2013).

[25] F. Kümmel, B. ten Hagen, R. Wittkowski, I. Buttinoni, R. Eichhorn, G. Volpe, H. Löwen, and C. Bechinger, Phys. Rev. Lett. **110**, 198302 (2013).

[26] W. E. Uspal, M. N. Popescu, S. Dietrich, and M. Tasinkevych, Soft Matter **11**, 434 (2015).

[27] M. S. D. Wykes, J. Palacci, T. Adachi, L. Ristroph, X. Zhong, M. D. Ward, J. Zhang, and M. J. Shelley, Soft Matter **12**, 4584 (2016).

[28] A. Aubret, S. Ramananarivo, and J. Palacci, Curr. Opin. Colloid Interface Sci. **30**, 81 (2017).

[29] M. Y. B. Zion, X. He, C. C. Maass, R. Sha, N. C. Seeman, and P. M. Chaikin, Science **358**, 633 (2017).

[30] M. N. Popescu, W. E. Uspal, C. Bechinger, and P. Fischer, Nano Lett. **18**, 5345 (2018).

[31] A. M. Brooks, S. Sabrina, and K. J. M. Bishop, Proc. Natl. Acad. Sci. USA **115**, E1090 (2018).

[32] A. Aubret and J. Palacci, Soft Matter **14**, 9577 (2018).

[33] M. Lisicki, S. Y. Reigh, and E. Lauga, Soft Matter **14**, 3304 (2018).

[34] A. M. Brooks, M. Tasinkevych, S. Sabrina, D. Velegol, A. Sen, and K. J. M. Bishop, Nat. Commun. **10**, 495 (2019).

[35] J. G. Lee, A. M. Brooks, W. A. Shelton, K. J. M. Bishop, and B. Bharti, Nat. Commun. **10**, 2575 (2019).

[36] S.-Y. Reigh, M.-J. Huang, H. Löwen, E. Lauga, and R. Kapral, Soft Matter **16**, 1236 (2020).

[37] M. Mijalkov and G. Volpe, Soft Matter **9**, 6376 (2013).

[38] J. Su, H. Jiang, and Z. Hou, Soft Matter **15**, 6830 (2019).

[39] D. Levis, I. Pagonabarraga, and B. Liebchen, Phys. Rev. Research **1**, 023026 (2019).

[40] T. Barois, J.-F. Boudet, J. S. Lintuvuori, and H. Kellay, Phys. Rev. Lett. **125**, 238003 (2020).

[41] J.-j. Liao, X.-q. Huang, and B.-q. Ai, J. Chem. Phys. **148**, 094902 (2018).

[42] A. Aubret, M. Youssef, S. Sacanna, and J. Palacci, Nat. Phys. **14**, 1114 (2018).

[43] J. R. Gomez-Solano, A. Blokhuis, and C. Bechinger, Phys. Rev. Lett. **116**, 138301 (2016).

[44] J. L. Aragones, S. Yazdi, and A. Alexander-Katz, Phys. Rev. Fluids **3**, 083301 (2018).

[45] C. Lozano, J. R. Gomez-Solano, and C. Bechinger, Nat. Mater. **18**, 1118 (2019).

[46] K. Qi, E. Westphal, G. Gompper, and R. G. Winkler, Phys. Rev. Lett. **124**, 068001 (2020).

[47] L. Theeyancheri, S. Chaki, N. Samanta, R. Goswami, R. Chelakkot, and R. Chakrabarti, Soft Matter **16**, 8482 (2020).

[48] C. Abaurrea-Velasco, C. Lozano, C. Bechinger, and J. de Graaf, Phys. Rev. Lett. **125**, 258002 (2020).

[49] N. Narinder, C. Bechinger, and J. R. Gomez-Solano, Phys. Rev. Lett. **121**, 078003 (2018).

[50] C. Krüger, G. Klös, C. Bahr, and C. C. Maass, Phys. Rev. Lett. **117**, 048003 (2016).

[51] M. Morozov and S. Michelin, Soft Matter **15**, 7814 (2019).

[52] J. R. Blake, J. Fluid Mech. **46**, 199 (1971).

[53] J. L. Moran and J. D. Posner, Annu. Rev. Fluid Mech. **49**, 511 (2017).

[54] See Supplemental Material at http://link.aps.org/supplemental/10.1103/PhysRevE.104.044607 for more information on the numerical method and on the comparison with the experiments, which includes Refs. [49,58,66–69].

[55] J. L. Anderson, Annu. Rev. Fluid Mech. **21**, 61 (1989).

[56] S. Michelin and E. Lauga, J. Fluid Mech. **747**, 572 (2014).

[57] R. Golestanian, T. Liverpool, and A. Ajdari, New J. Phys. **9**, 126 (2007).

[58] J. R. Gomez-Solano, S. Samin, C. Lozano, P. Ruedas-Batuecas, R. van Roij, and C. Bechinger, Sci. Rep. **7**, 14891 (2017).

[59] R. G. Larson, E. S. G. Shaqfeh, and S. J. Muller, J. Fluid Mech. **218**, 573 (1990).

[60] A. Varshney and V. Steinberg, Phys. Rev. Fluids **2**, 051301(R) (2017).

[61] L. W. Rogowski, J. Ali, X. Zhang, J. N. Wilking, H. C. Fu, and M. J. Kim, Nat. Commun. **12**, 1116 (2021).

[62] S. Saad and G. Natale, Soft Matter **15**, 9909 (2019).

[63] A. I. Campbell, S. J. Ebbens, P. Illien, and R. Golestanian, Nat. Commun. **10**, 3952 (2019).

[64] J. Simmchen, J. Katuri, W. E. Uspal, M. N. Popescu, M. Tasinkevych, and S. Sánchez, Nat. Commun. **7**, 10598 (2016).

[65] T. Pedley, IMA J. Appl. Math. **81**, 488 (2016).

[66] R. Williams and A. M. Goodman, Appl. Phys. Lett. **25**, 531 (1974).

[67] J. Francois, D. Sarazin, T. Schwartz, and G. Weill, Polymer **20**, 969 (1979).

[68] F. Taherian, V. Marcon, N. F. A. van der Vegt, and F. Leroy, Langmuir **29**, 1457 (2013).

[69] T. Werder, J. H. Walther, R. L. Jaffe, T. Halicioglu, F. Noca, and P. Koumoutsakos, Nano Lett. **1**, 697 (2001).